Available online at www.sciencedirect.com

ScienceDirect

Procedia Structural Integrity 44 (2023) 283–290

Structural Integrity Procedia

www.elsevier.com/locate/procedia

XIX ANIDIS Conference, Seismic Engineering in Italy

Fragility curves for reinforced concrete frames characterised by different regularity

Giovanni Smiroldo[a]*, Marco Fasan[a], Claudio Amadio[a]

[a]*University of Trieste, Department of Engineering and Acrhitecture, Via Alfonso Valerio 6/1, 34127 Trieste, Italy*

Abstract

This paper presents a comparison between fragility curves developed for regular and non-regular reinforced frames. Three 3D reinforced concrete multi-story frames characterised by different regularity are analysed. These fragility curves are developed through the "Cloud Analysis" procedure, which evaluates the structural response via Non-Linear Time History Analysis (NLTHA).

Both maximum inter-story drift and maximum chord-rotation demand/capacity ratio are used as Engineering Demand Parameters, in which the chord-rotation capacity is calculated according to the Italian Code. To fully develop the fragility curves, both structure-independent and structure-dependent scalar intensity measures are selected among the most referred in practice and literature.

This work shows the influence of regularity on the damage levels of the three buildings. Furthermore, it shows the uncertainties caused by the selection criteria for EDP thresholds, which are necessary for a correct representation of the Limit State.

© 2023 The Authors. Published by Elsevier B.V.
This is an open access article under the CC BY-NC-ND license (https://creativecommons.org/licenses/by-nc-nd/4.0)
Peer-review under responsibility of the scientific committee of the XIX ANIDIS Conference, Seismic Engineering in Italy.

Keywords: Fragility curves; RegularityuCloud Analysis; Intensity Measure, Engeneering Demand Parameter;

* Corresponding author
E-mail address: giovanni.smiroldo@phd.units.it

2452-3216 © 2023 The Authors. Published by ELSEVIER B.V.
This is an open access article under the CC BY-NC-ND license (https://creativecommons.org/licenses/by-nc-nd/4.0)
Peer-review under responsibility of the scientific committee of the XIX ANIDIS Conference, Seismic Engineering in Italy.
10.1016/j.prostr.2023.01.037

1. Introduction

It is commonly accepted that irregularities in structure configuration affect seismic performance and structural dynamic response. Structural regularity aims to give constructions a uniform behaviour to avoid concentrated stresses. In general, a building is considered in-plant and in-height regular when fundamental translational modes rule its dynamic behaviour, reducing torsional effects. The irregularity-related requirements found in codes and standards generally reflect the best judgment of practitioners and academics based primarily on anecdotal observations and fairly simple linear static and linear dynamic analyses, without explicit consideration of collapse probability (FEMA 2018).

To evaluate torsional contributions to seismic response, in this work, fragility curves are developed for three RC buildings, investigated via Non-Linear Time History Analysis (NLTHA). Furthermore, fragility allows to take into consideration collapse prevention probability. There are several procedures to develop fragility functions based on NLTHAs such as Incremental Dynamic Analysis (IDA) (Vamvatsikos and Cornell 2002), and Cloud Analysis (CA) (Luco and Cornell 2007; Jalayer et al. 2015, 2017). In this work, the Cloud Analysis procedure is selected. The seismic input consists in a set of unscaled real recorded accelerograms.

Fragility curves are evaluated among a set of scalar intensity measures, both structure-independent and structure-dependent.

To assess structural damage, this paper considers two Engineering Demand Parameters (EDP): the maximum Inter-Storey Drift Ratio and the maximum Chord-Rotation Demand/Capacity Ratio. These two EDP are chosen to better understand the real behaviour and to make a comparison between the fragility curves defined for each one of them. The use of two EDPs allows for a validation of results.

2. Reference structures and non-linear time history analysis settings

The reference structures adopted are three multi-storey reinforced concrete frames with different levels of regularity. The first structure, called “Regular Frame” (“RF”) is characterised by a square plan of 15m width, subdivided in three bays of 5m length each. A strength class C20/25 was adopted for concrete, while steel bars type B450C (as defined by the Italian Building Code) were used.

Using a response spectrum analysis to obtain the maximum stress values, beams and columns are designed according to the Italian Building Code (NTC18) considering a high seismicity area, a low ductility class (Class B) and adopting a behaviour factor equal to 3.9. The weak beam/strong column capacity design criteria are applied and shear forces in members are evaluated from the flexural capacity of their critical regions preventing any shear weak failure. Floors are considered as rigid diaphragms and a fixed support is applied at the base nodes.

To quantify the levels of irregularity of the building, it is used the Torsional Irregularity Ratio (TIR) (ASCE/SEI 7-16, 2014), defined as the ratio of the maximum drift at building’s edge to the average drift. To obtain a suitable in plant and in height non-regularity, building parts were removed, i.e. beam elements and column elements. Thus, two more buildings are derived, characterised by different levels of regularity, called “Non-Regular Frame 1” (NRF1) and “Non-regular Frame 2” (NRF2). They are redesigned according to the Italian Building Code. The TIR of the structures are shown in Table 1:

Table 1 - TIR

	RF	NRF1	NRF2
TIR	1.0	1.15	1.3

The reference structures are shown in Figure 1 and Figure 2.

Tables 2, Table 3, and Table 4 summarize vibrational modes properties and mass participation ratios (MPR) of the designed structures:

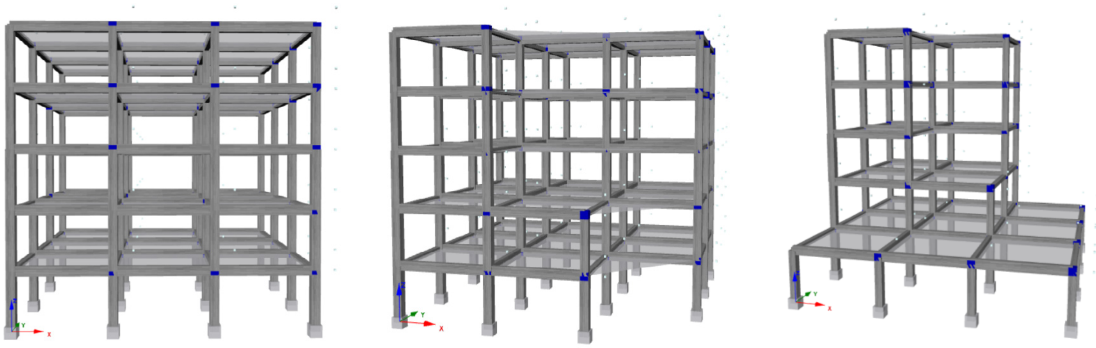

Fig. 1 - a) Regular Frame; b) Non-Regular Frame 1; c) Non-Regular Frame 2

Table 2 –Vibrational periods and masses

Regular Frame 'RF'				
Mode	Period [s]	[MPRx]	[MPRy]	[MPRz]
1	0.956	0.00%	**80.03%**	0.00%
2	0.857	0.00%	0.00%	**80.74%**
3	0.745	**82.17%**	0.00%	0.00%
Non-Regular Frame 1 ‘NRF1’				
1	0.986	0.01%	**76.78%**	1.13%
2	0.839	1.97%	1.08%	**75.54%**
3	0.730	**78.70%**	0.01%	1.40%
Non-Regular Frame 2 ‘NRF2’				
1	1.014	0.33%	**63.84%**	5.16%
2	0.738	30.11%	1.88%	**34.90%**
3	0.658	**40.84%**	0.28%	15.41%

Non-linear time history analyses (NLTHAs) are performed using the software Seismostruct (Seismosoft 2022). Both material and geometrical non-linearities are included. Material non-linearities are accounted for using a force-based inelastic frame element (*infrmFB*), that adopts a diffused plasticity model through a fibre-section discretization. A total number of 5 integration sections with 150 discretized fibres is used for each beam element.

To simulate the rigid slab at each floor, “rigid diaphragm constraints” have been used. As described in the Seismostruct Manual, the simultaneous use of diffused plasticity model and rigid diaphragm constraint will generate very high fictitious axial internal forces in horizontal elements. To prevent this interaction, beams are released from the axial constraint through rigid links to which is given no axial stiffness and infinite stiffness in the other degrees of freedom, as described in Barbagallo et al (2019).

A Rayleigh damping is used, for which it is necessary to define two vibrational periods and a target damping factor for each of the two chosen modes. The two periods are chosen to avoid overdamping of higher mode and elongation of modes due to plastic deformations. They consist of 1.5 times the first vibrational period and the period that leads to a cumulative mass participation ratio of 90%. The target damping factor is 3% (ASCE 2014). The Hilber – Hughes – Taylor integration scheme is used.

3. Seismic input and intensity measure selection

Fragility is usually evaluated through structural responses estimated via Non-Linear Time History Analysis (NLTHA).

The Cloud Analysis procedure is selected to develop fragility curves due to its reduced computational cost of approach (Mattei et al, 2021), and since it is based on the use of unscaled records avoiding possible biases introduced by scaling (Luco and Bazzurro, 2007; Zacharenaki et al., 2014). In this work, it is used a set of 62 unscaled ground-motion records, chosen from the European Strong Motion Database (Luzi et al, 2020).

When adopting this method for fragility evaluation, few points should be considered (Jalayer et al., 2017):

- The records should cover a wide range for the selected IM;
- A significant number of records (about 20-30%) should lead to an exceedance of the selected EDP capacity for the selected performance level;
- Not more than 10% of records from the same event should be selected.

Figure 2 shows the Moment-Magnitude/Distance correlation of the selected record:

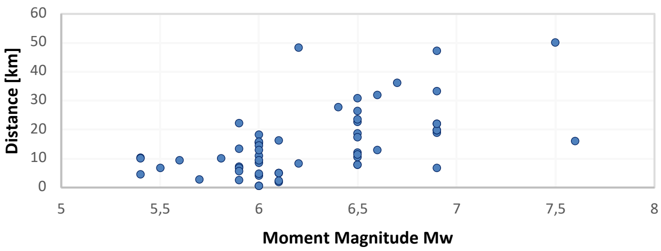

Fig. 2 - Magnitude - Distance correlation of the seismic input

To compose the fragility curves, each record is represented by the intensity measures combined in the horizontal components. Boore (2010) assess that it is not precautionary to use the raw geometric mean for combining the horizontal components of the records. Thus, he proposes a new bi- dimensional parameter of the intensity measures of ground motion records, called RotD100. It is defined as the maximum mean value over all possible nonredundant angles. In this work, RotD100 is used for each intensity measure.

To develop fragility curves, both structure-independent and structure-dependent scalar intensity measures are selected among the most referred in practice and literature: the structure-independent ones (i.e., those who do not depend on the vibrational properties of the structure) are the Peak Ground Acceleration (PGA), Housner Intensity, and the Cumulative Absolute Velocity (Reed and Kassawara, 1990). The latter is expressed in Eq. (1):

$$CAV = \int \left| a_g(t) \right| dt \qquad \text{Eq. (1)}$$

For structure-dependent intensity measures, one of the most used IMs is the spectral acceleration at first mode $S_a(T_1)$. As the reference structure and NLTHAs are 3D, the IM should account for the main vibrational properties in both directions. Hence, spectral acceleration is here evaluated at a mean period $T1m$ defined as the average of the values of the fundamental periods in each direction (FEMA 2018), expressed in Eq. (2):

$$S_a(T_{1m}) = S_a\left(\frac{T_{1x}+T_{1y}}{2}\right) \qquad \text{Eq. (2)}$$

Another IM used is the Pseudo Spectral Velocity (PSV). It is derived from the components of Spectral Displacement S_d, which is given by the ESM flat-file. Eventually, it is multiplied for the frequency of the reference structure in both directions, as expressed in Eq. (3) and Eq. (4):

$$\omega = \frac{2\pi}{T} \qquad \text{Eq. (3)}$$

$$PSV = S_d * \omega \qquad \text{Eq. (4)}$$

One the most referred IMs in literature is the Housner Intensity, calculated as the integral of the response spectrum in terms of pseudo-velocity in the interval between 1s and 2.5s, as expressed in Eq. (5). This IM is correlated to the potential damage provided by the reference record, and it is structure-independent:

$$Housner = \int_{0.1}^{2.5} PSV\ (T, \xi = 0.05) dt \qquad \text{Eq. (5)}$$

The last IM used in this work is the Modified Acceleration Spectrum Intensity (MASI), calculated as the integral of the response spectrum in terms of pseudo-acceleration and derived from the spectral displacement multiplied for the square of the frequency of the reference structure, expressed by Eq. (6) and Eq. (7):

$$PS_a = S_d * \omega^2 \qquad \text{Eq. (6)}$$

$$MASI = \int_{0.1}^{1} PS_a\ (T, \xi = 0.05) dt\mathrm{q} \qquad \text{Eq. (7)}$$

Each IM is represented by the RotD100 parameter, which is the RotD at the 100th percentile.

4. Engineering Demand Parameters selection

Generally, structural damage is correlated with inter-storey drift ratio (IDR) occurring at each floor, that is a global parameter. To use a unique directionless value, the resultant inter-storey drift is calculated via SRSS combination of the IDR in the two orthogonal directions. Finally, the maximum inter-storey drift (MIDR) observed in the building is adopted as a single EDP to define the level damage reached in the structures.

In this work, a more sophisticated EDP is used and compared with the maximum IDR. It is the local parameter Chord-rotation Capacity-Demand Ratio (DCR), calculated for each local axis of horizontal elements ends defined by the Italian Building Code (C.S.LL.PP 2018) at C8.7.2.1, as the following eq. (8):

$$\theta_u = \frac{1}{\gamma_{el}} 0.016 \cdot (0.3^{\nu}) \left[\frac{\max(0.01;\omega')}{\max(0.01;\omega)} f_c\right]^{0.225} \left(\frac{L_V}{h}\right)^{0.35} 25^{\left(\alpha\rho_{sx}\frac{f_{yw}}{f_c}\right)} (1.25^{100\rho_d}) \qquad \text{Eq. (8)}$$

Finally, the maximum chord-rotation capacity demand ratio (MDCR) observed in the building is adopted as a single EDP.

5. Fragility curves development

Fragility curves allow engineers to estimate the probability of attainment of a definite damage state (e.g., Collapse Limit State) given a specified magnitude of an Engineering Demand Parameter, EDP (e.g., inter-storey drift ratio). As mentioned in the § 3, in this work fragility functions are developed via Cloud Analysis Procedure, using the regression line intercept “b” and slope “a” within the bi-logarithmic plane. The curves are presented in the form of cumulative distribution function by Eq. (9) with respect to the IM.

$$P\left[EDP \geq EDP_{pl} | IM\right] = 1 - \Phi\left(\frac{\ln(EDP_0) - \ln(aIM^b)}{\sigma}\right) = \Phi\left(\frac{\ln(IM) - \ln(\lambda)}{\zeta}\right) \qquad \text{Eq. (9)}$$

Where:

- aIM^b is the equation of the regression line of the reference correlation;
- σ is the standard deviation of the reference correlation;
- $\lambda = \frac{\ln(EDP_0)-\ln(a)}{b}$;
- $\zeta = \sigma/b$.

In order to generate fragility curves for MIDR and MDCR two performance level are considered, (NTC2018): Life Safety (LS) and Collapse Prevention (CP).

EDP Life Safety thresholds are calculated as ¾ of Collapse Prevention thresholds. For MIDR the assumed capacity thresholds are identified by means of pushover analysis carried out for each structure, using the chord-rotation demand/capacity as collapse control parameter. MDCR Collapse Prevention threshold is obtained every time the chord-rotation demand reaches the chord-rotation capacity. Table 5 summarises the thresholds:

Table 3 - EDPs Thresholds

EDP Threshold			
	RF	NRF1	NRF2
MIDR CP	5%	5%	5%
MIDR LS	3.75%	3.75%	3.75%
MDCR CP	1	1	1
MDCR LS	075	0.75	0.75

6. Results

IMs and EDPs correlations are made. In order to develop fragility curves the correlations are made in a bi-logarithmic scale. The best correlations between IM and EDP are characterised by lower standard deviations, as shown in the Figure 3:

Correlations (MIDR - IM)	**RF**	**NRF1**	**NRF2**
ln(MIDR)-ln(RotD100_SaT1)	0.43	0.43	0.43
ln(MIDR)-ln(RotD100_pga)	0.50	0.48	0.47
ln(MIDR)-ln(RotD100_PSV)	0.43	0.43	0.43
ln(MIDR)-ln(RotD100_CAV)	0.48	0.47	0.47
ln(MIDR)-ln(RotD100_Housner)	0.18	0.19	0.19
ln(MIDR)-ln(RotD100_MASI)	0.45	0.44	0.42

Correlations (MDCR - IM)	**RF**	**NRF1**	**NRF2**
ln(MDCR)-ln(RotD100_SaT1)	0.53	0.50	0.45
ln(MDCR)-ln(RotD100_pga)	0.61	0.57	0.50
ln(MDCR)-ln(RotD100_PSV)	0.53	0.50	0.45
ln(MDCR)-ln(RotD100_CAV)	0.58	0.55	0.51
ln(MDCR)-ln(RotD100_Housner)	0.26	0.22	0.21
ln(MDCR)-ln(RotD100_MASI)	0.55	0.52	0.45

Fig. 3 - Standard deviations

This table shows that the best correlation is between both EDP and the Housner Intensity. For simplicity it will be used as the reference for the fragility curves results. The correlations between EDPs and Housner Intensity are shown in Figure 4:

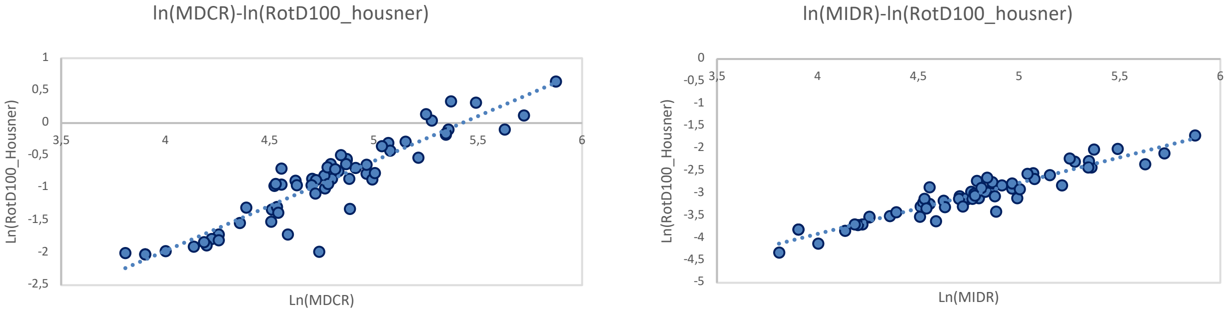

Fig. 4 - a) MDCR correlation; b) MIDR correlation

Figure 5 shows the fragility curves obtained:

Fig. 5 - a) MDCR CP Fragil

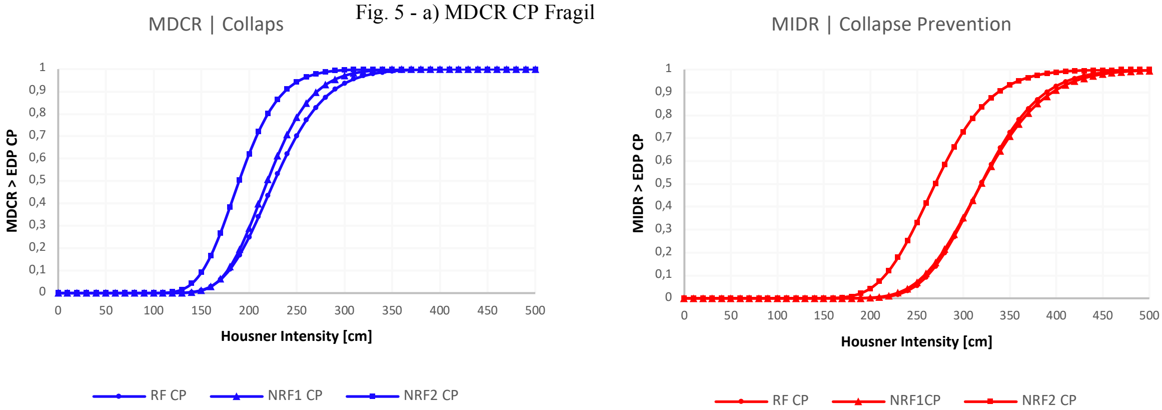

These pictures show a clear difference in the dynamic response of the analyzed buildings: the RF structure suffers less displacements than the NRF2 structure, as shown in Figure 5. The highest deformability of the NRF2 structure derives from the higher non-regularity and relative torsional effects.

The threshold selection is a key factor for the right construction of the fragility curves. The MIDR thresholds are identified via pushover analysis of the buildings, although pushover analyses are not recommendable for studying buildings characterised by high levels of non-regularity, since the first vibration mode is not well defined. The implementation of the chord-rotation capacity as an Engineering Demand Parameter has the aim to implicitly consider the Collapse Prevention Limit State reached by every element of the reference structure. This avoids the necessity to assess non-regular structure capacity thresholds by means of improper method such as pushover analysis and its relative uncertainty. Thus, the fragility curves constructed with the MDCR as EDP are more representative of the real behaviour of the buildings.

The fragility curves show another difference: there is a noteworthy difference in dynamic response of the structures between using MDCR instead of MIDR. Given that MIDR thresholds are determined via pushover analysis which possesses approximations, the curves obtained with MDCR as EDP induces to a more reliable reading.

7. Discussion and future studies

This paper showed that fragility curves can detect and evaluate the influence of non-regularity (and consequential torsional effects) on NTC2018 defined buildings under seismic loads. Moreover, fragility curves obtained with MDCR as EDP are more reliable.

Finally, the Cloud Analysis procedure assures low computational costs and avoid possible biases derived from scaled accelerograms.

However, Cloud Analysis procedure presents two main problems. Firstly, there are few recorded accelerograms capable of inducing collapse in modern-code conforming seismic designed buildings. This issue is particularly important if the fragility analysis aims to evaluate the effects of collapses. Secondly, it is not possible to perform seismic vulnerability analysis via Cloud Analysis in specific sites, again because there are not enough recorded accelerograms to make it viable.

In this framework, future development should be oriented to the use of physics-based ground motion simulations. Their reliability has already been proved in the study of site-specific hazard assessment and they allow for a correct representation of seismic input (Hassan et al, 2020; Chieffo et al, 2021).

Further application will regard the evaluation of the vulnerability under seismic sequences of the reference structures studied in this work, combining the methodology proposed by Rinaldin et al (2020) with physics-based ground motion simulations.

References

ASCE, 2014. Seismic Evaluation and Retrofit of Existing Buildings. American Society of Civil Engineers, Reston, VA.

Barbagallo F., Bosco M., Marino E. M., Rossi P.P., 2019. On the fibre modelling of beams in RC framed buildings with rigid diaphragm. Department of Civil Engineering and Architecture, University of Catania, Catania, Italy.

Boore D. M, 2010. Orientation-independent, nongeometric-mean measures of seismic intensity from two horizontal components of motion. Bulletin of the Seismological Society of America 100:1830–1835. doi: 10.1785/0120090400.

C.S.LL.PP; 2018. Norme tecniche per le costruzioni. Rome, Italy.

Chieffo, N.; Fasan, M.; Romanelli, F.; Formisano, A.; Mochi G., 2021. Physics-Based Ground Motion Simulations for the Prediction of the Seismic Vulnerability of Masonry Building Compounds in Mirandola (Italy). Buildings 2021, 11, 667. https://doi.org/10.3390/buildings 11120667.

FEMA, 2018. Seismic Performance Assessment of Buildings. FEMA P-58-1. Washington, D.C, U.S.A.

Jalayer F., De Risi R., Manfredi G., 2015: Bayesian Cloud Analysis. Efficient structural fragility assessment using linear regression. Bull.Earthq.Eng., 13, 1183:1203, doi: 10.1007/s10518-014-9692-z.

Jalayer F., Ebrahimian H., Miano A., et al, 2017. Analytical fragility assessment using unscaled ground motion records. Earthquake Engineering and Structural Dynamics 46:2639–2663. doi: 10.1002/eqe.2922.

Hassan H.M., Fasan M., Sayed M.A., et al., 2020. Site-specific ground motion modeling for a historical Cairo site as a step towards computation of seismic input at cultural heritage sites. Engineering Geology 268:105524. doi: 10.1016/j.enggeo.2020.105524.

Luco N., Bazzurro P., 2007. Does amplitude scaling of ground motion records result in biased nonlinear structural drift responses? Earthquake Engineering & Structural Dynamics 36:1813–1835. doi: 10.1002/eqe.695

Luco N., Cornell C. A., 2007. Structure-specific scalar intensity measures for near-source and ordinary earthquake ground motions. Earthquake Spectra 23:357–392. doi: 10.1193/1.2723158.

Luzi L., Lanzano G., Felicetta C., D'Amico M. C., Russo E., Sgobba S., Pacor F., & ORFEUS Working Group 5, 2020. Engineering Strong Motion Database (ESM) (Version 2.0). Istituto Nazionale di Geofisica e Vulcanologia (INGV). https://doi.org/10.13127/ESM.2

Mattei S., Fasan M., Bedon C, 2021. On the Use of Cloud Analysis for Structural Glass Members under Seismic Events. Sustainability 2021, 13, 9291. https://doi.org/10.3390/su13169291.

Reed J. W., Kassawara R. P., 1990. A criterion for determining exceedance of the operating basis earthquake. Nuclear Engineering and Design 123:387–396. doi: 10.1016/0029-5493(90)90259-Z.

Rinaldin G., Fasan M., Sancin L., Amadio C., 2020. On the behaviour of steel CBF for industrial buildings subjected to seismic sequences. Structures 28 (2020) 2175-2187. https://doi.org/10.1016/j.istruc.2020.10.050.

Seismosoft, 2022. SeismoStruct 2022 – A computer program for static and dynamic nonlinear analysis of framed structures.

Vamvatsikos D., Cornell C. A., 2002. Incremental dynamic analysis. Department of Civil and Environmental Engineering. Stanford University, U.S.A.

Zacharenaki A., Fragiadakis M., Assimaki D., Papadrakakis M.,2014. Bias assessment in Incremental Dynamic Analysis due to record scaling. Soil Dynamics and Earthquake Engineering 67:158–168. doi: 10.1016/j.soildyn.2014.09.007.